Combinations of Bevacizumab and Erlotinib Show Activity in Colorectal Cancer Independent of RAS Status

Paul Mésange, Anaïs Bouygues, Nathalie Ferrand, Michèle Sabbah, Alexandre Escargueil, Ariel Savina, Benoist Chibaudel, Christophe Tournigand, Thierry André, Aimery de Gramont, et al.

Combinations of Bevacizumab and Erlotinib Show Activity in Colorectal Cancer Independent of *RAS* Status

Paul Mésange[1,2,3], Anaëlle Bouygues[1,2,3], Nathalie Ferrand[1,2,3], Michèle Sabbah[1,2,3,4], Alexandre E. Escargueil[1,2,3], Ariel Savina[5], Benoist Chibaudel[1,2,6], Christophe Tournigand[7,8], Thierry André[1,2,3,9], Aimery de Gramont[1,2,6], and Annette K. Larsen[1,2,3,4]

Abstract

Purpose: There is extensive cross-talk between VEGF- and EGFR-pathway signaling in colorectal cancer. However, combinations of VEGF- and EGFR-targeted monoclonal antibodies (mAb) show disappointing activity, in particular for patients with mutant *RAS*. Previous results show that tyrosine kinase inhibitors (TKI) can be active in colorectal cancer models resistant to mAbs. This prompted us to examine whether the activity of bevacizumab can be increased by combination with erlotinib.

Experimental Design: The antitumor activity of bevacizumab, erlotinib, and their combination was determined in colorectal models with different *RAS* status and bevacizumab sensitivity. EGFR/VEGF pathway activation was characterized by immunohistochemistry, Western blot, and ELISA assays. The influence of cetuximab and erlotinib on EGF-mediated migration and the EGFR–EGF ligand feedback loop was established in colorectal cancer cell lines with different *RAS* status.

Results: The addition of erlotinib increased bevacizumab activity in all models independent of *RAS* status. Bevacizumab exposure was accompanied by marked EGFR activation in tumor cells as well as in tumor-associated endothelial cells (TECs) and resulted in strong accumulation of intracellular EGFR, which could be attenuated by erlotinib. In cellular models, erlotinib was able to attenuate EGF-mediated functions in all cell lines independent of *RAS* status while cetuximab only showed activity in *RAS* wild-type cells.

Conclusions: These results should provide a molecular framework to better understand the increased activity of the bevacizumab–erlotinib combination, compared with bevacizumab alone, in the GERCOR DREAM phase III clinical trial. Differential activity of mAbs and TKIs targeting the same signaling pathway is likely applicable for other tumor types. colorectal

Introduction

The epidermal growth factor receptor (EGFR) and the vascular endothelial growth factor (VEGF) pathways are validated targets for treatment of patients with metastatic colorectal cancer (mCRC). There is extensive cross-talk between these two signaling pathways (1) and combinations of VEGF(R) and EGFR-directed compounds have consistently shown at least additive activity in preclinical models (2). However, the results of clinical trials were disappointing because the addition of EGFR-targeted monoclonal antibodies (mAb) to bevacizumab plus chemotherapy was no better, in terms of overall survival, than bevacizumab plus chemotherapy alone, even for patients with wild-type *RAS* tumors, and was detrimental, in terms of progression-free survival, for most patients with *KRAS*-mutant tumors (3, 4).

To determine if these disappointing results were pathway- or agent-related, we compared the antitumor activity of two mAbs with two small molecule tyrosine kinase inhibitors (TKI) in the same colorectal cancer xenograft models (5). The results showed that the combination of the two antibodies was no more active than either agent alone while the combination of the TKIs showed synergistic antitumor activity. Unexpectedly, the TKI combination was also active in colorectal cancer models with mutant *RAS* status (5), indicating that mutant *RAS* may not be a limiting factor for EGFR-directed TKIs like it is for the mAbs (6–8). These findings provided the rationale for the current study, which shows that erlotinib enhances the *in vivo* activity of bevacizumab independent of *RAS* status. We further demonstrate a differential activity of cetuximab and erlotinib on EGFR-mediated functions in colorectal cancer cells revealing fundamental differences between mAbs and TKIs targeting the same pathway.

[1]Cancer Biology and Therapeutics, Centre de Recherche Saint-Antoine (CRSA), Paris, France. [2]Institut National de la Santé et de la Recherche Médicale (INSERM) U938, Paris, France. [3]Institut Universitaire de Cancérologie (IUC), Faculté de Médecine, Sorbonne Université, Paris, France. [4]Centre National de la Recherche Scientifique (CNRS), Paris, France. [5]Roche Scientific Partnerships, Boulogne-Billancourt, France. [6]Department of Medical Oncology, Institut Hospitalier Franco-Britannique, Levallois-Perret, France. [7]Department of Medical Oncology, Assistance Publique-Hôpitaux de Paris, Hôpital Henri Mondor, Créteil, France. [8]Université Paris Est, Créteil, France. [9]Department of Medical Oncology, Assistance Publique-Hôpitaux de Paris, Hôpital Saint-Antoine, Paris, France.

Note: Supplementary data for this article are available at Clinical Cancer Research Online (http://clincancerres.aacrjournals.org/).

Corresponding Author: Annette K. Larsen, Cancer Biology and Therapeutics, Kourilsky Research Building 1st floor, Hôpital Saint-Antoine, 184 rue du Faubourg Saint-Antoine, F75571 PARIS Cedex 12 France. Phone: 33-1-49-28-46-87; E-mail: annette.larsen@sorbonne-universite.fr

Translational Relevance

The epidermal growth factor receptor (EGFR) and the vascular endothelial growth factor (VEGF) pathways are validated targets for treatment of patients with metastatic colorectal cancer. However, combinations of monoclonal antibodies targeting both pathways show disappointing results. We here show that combinations of bevacizumab and erlotinib, a small-molecule EGFR inhibitor, show activity in colorectal cancer models independent of *RAS* status and bevacizumab resistance. Bevacizumab exposure was accompanied by intracellular accumulation of active, phosphorylated EGFR in both tumor cells and tumor-associated endothelial cells and could be attenuated by erlotinib. We further demonstrate differential activity of cetuximab and erlotinib on EGFR-mediated functions in colorectal cancer cells as a function of *RAS* status revealing fundamental differences between mAbs and TKIs targeting the same pathway. These findings may be applicable for other tumor types as well.

Materials and Methods

Drugs

Bevacizumab (Avastin) was provided by Roche, cetuximab was from Merck, and erlotinib (Tarceva) was purchased from LC Laboratories.

Tumor cells

Colorectal cancer cells were maintained in cell culture as described previously (9). SW48, LS174T, and DLD-1 colorectal cancer cells were a kind gift from Richard Hamelin (Saint-Antoine Research Center, Paris, France), while SW480 and LIM1215 cells were purchased from American Type Culture Collection. HT-29, CoLo205, and SW620 cells were kindly provided by Richard Camalier (NCI, Bethesda, MD) while HCT-116 cells were a generous gift from Bert Vogelstein (John Hopkins, Baltimore, MD). Upon defreezing and prior to each animal experiment, cells were monitored for *mycoplasma* contamination using the MycoAlert Mycoplasma Detection Kit (Lonza). Cells were characterized by next-generation sequencing of 50 cancer-related genes using the Ion AmpliSeq Cancer Hotspot Panel v2 (Thermo Fisher Scientific) and were replaced after 3 months in culture.

In vivo studies

The antitumor effects of bevacizumab, erlotinib, and their combination were evaluated in athymic mice (female NMRI-Foxn1 nu/nu, 6 weeks old) from Taconic bearing SW48, HT-29, or SW620 xenografts. Two to 5 million cells were injected into the right flank, and the treatments were started when the tumors were palpable. Animals were weighed daily and the tumor size was determined three times per week (10). Tumor volumes (mm^3) were calculated according to the formula: [(length $\times$ width^2)/2]. Boxplot analysis was carried out using the GraphPad prism 6.04 software (GraphPad). Treated/control (T/C) values were calculated as follows: average tumor volume of treated animals/average tumor volume of control animals $\times$ 100. Animals were treated according to institutional guidelines and the protocol was approved by the institutional ethics committee for animal experimentation (Institutional Animal Care and Use Committee).

Antibodies

The following antibodies were used for immunohistochemistry (IHC) analysis: anti-CD31 (#550274, BD Bioscience) to determine the vascular density, anti-VEGF-A (sc-152, Santa Cruz Biotechnology, CliniSciences), anti-phospho-VEGFR1 (07-758, Millipore) that recognizes phospho-Tyr 1213, anti-phospho-VEGFR2 (# 2478, Cell Signaling Technology, Ozyme) that recognizes phospho-Tyr 1175, anti-phospho-EGFR (sc-12351, Santa Cruz Biotechnology) that recognizes phospho-Tyr 1173, anti-EGFR (sc-03, Santa Cruz Biotechnology), and anti-amphiregulin (AF262, R&D System). The relevant Cy3-conjugated secondary antibodies were obtained from Jackson ImmunoResearch.

The following antibodies were used for Western blot analysis: anti-phospho-EGFR antibody (#3777, Cell Signaling Technology) that recognizes Tyr1068 EGFR, anti-EGFR antibody (sc-03, Santa Cruz Biotechnology) and anti-actin-HRP antibody (sc-1615, Santa Cruz Biotechnology) followed by incubation with the appropriate horseradish peroxidase-conjugated secondary antibodies (Cell Signaling Technology).

Immunohistochemistry

Biomarker analysis was carried out with tumors collected after 4 weeks of treatment and processed for immunohistochemistry (IHC) analysis. All images were captured by a fluorescence microscope, and the fluorescence intensities were determined by the MetaMorph software (Universal Imaging Corporation) for quantitative image analysis. When indicated, tumors were counterstained by 4^0,6-diamidino-2-phenylindole to reveal the nuclei of individual cells. For the quantitative analysis of the signal intensity, the data represent the average fluorescence intensity of treated tumors compared with the treatment intensity of control tumors and is the average of 6 fields/tumor for at least 3 different tumors. Blood vessel density is expressed as the CD31-positive area, in percentage of total and represent the averages of at least 6 fields/tumor for at least 3 different tumors.

For the determination of pEGFR expression by the TECs, double labeling was carried out for pEGFR and CD31 and the degree of colocalization was determined by semiquantitative analysis as illustrated in Fig. 4. Only blood vessels where the entire rim could be assessed were included in the analysis with at least 12 blood vessels per treatment.

ELISA assay and Western blot of xenograft samples

Tumor tissues were collected from untreated, frozen tumors (3 tumors per treatment) and protein extracts were prepared in RIPA buffer according to the manufacturer's instructions. VEGF levels were determined by Quantikine ELISA (# DVE00 and MMV00, R&D Systems) for human, tumor-derived VEGF and for murine, stroma-derived VEGF, respectively. Amphiregulin levels were determined by Quantikine ELISA (R&D Systems, # DAR00, human AREG). VEGFR1 and VEGFR2 levels were determined by DuoSet ELISA (DY321B and DYC1766, R&D Systems). The values represent the average of 3 independent experiments, each done in duplicate.

For Western blot, equal amounts of proteins (100 mg/lane) were loaded into SDS-PAGE gels, transferred onto nitrocellulose membranes and blotted with antibodies directed against phosphorylated and total EGFR. Protein expression was quantified by densitometric analysis of the immunoblots using Image Lab software (Bio-Rad) after normalization with b-actin.

ELISA assays of conditioned media

Cells were seeded and allowed to attach for 24 hours followed by 72- hours incubation in 5% FCS in the absence or presence of cetuximab (1 mg/mL) or erlotinib (3 mmol/L) as described (11). Conditioned media were collected and concentrated using Amicon ultracentrifugal filter units. The levels of secreted TGFa and amphiregulin were determined by Quantikine ELISA (R&D Systems, #DTGA00 for TGFa and #DAR00 for amphiregulin) according to the manufacturer's instructions. The values represent the average of 3 independent experiments, each done in duplicate.

Tumor cell migration

Cell migration was assessed by the Transwell assay (Boyden chamber, Dutscher) according to the manufacturer's instructions. Briefly, 50,000 to 100,000 cells in serum-free media with or without erlotinib or cetuximab were plated in the upper chamber on membranes with a pore size of 8 mm while the lower chamber contained culture media with EGF (20 ng/mL) as chemoattractant. After 6 hours, remaining cells were removed from the top side of the inserts whereas migrating cells on the bottom of the inserts were stained with Diff-Quik (Thermo Fischer Scientific), and all migrating cells were counted. Results are expressed as means ± SEM and represent triplicate samples from at least two independent experiments.

Statistical analysis

ANOVA was performed to determine the significance of observed differences between groups using the tool pack from Excel (Microsoft). *Post hoc* comparisons were made using Student paired *t* test using GraphPad Prism (GraphPad Software). Differences between two groups are presented as the mean ± SEM or mean ± SD as noted in the figure legends. All tests were two-sided and $P < 0.05$ were considered statistically significant.

Results

Erlotinib increases the antitumor activity of bevacizumab

Three different colorectal cancer xenograft models were used including SW48 [*RAS* wild-type (WT), bevacizumab sensitive], HT-29 (*RAS* WT, bevacizumab resistant), and SW620 (*RAS* mutant and bevacizumab sensitive; ref. 10). The antitumor activities of bevacizumab (1 mg/kg) and erlotinib were comparable for SW48 and SW620 xenografts with T/C values (average tumor volume of treated animals/average tumor volume of control animals × 100) of 55 and 54 for bevacizumab and 65 and 74 for erlotinib, respectively (Fig. 1). Combined treatment with bevacizumab and erlotinib increased the antitumor activity to T/C values of 33 and 39, respectively, which is significantly different from bevacizumab alone ($P < 0.01$). To confirm the activity of the bevacizumab þ erlotinib combination toward the *RAS*-mutant SW620 tumors, the experiment was repeated with a standard dose of bevacizumab (5 mg/kg). Under these conditions, the T/C value was 27 for bevacizumab alone and 16 for the combination ($P < 0.001$; Supplementary Fig. S1, top).

Bevacizumab exposure (5 mg/kg) was accompanied by modest tumor growth inhibition for HT-29 xenografts (T/C of 68), whereas erlotinib treatment was associated with unexpected strong antitumor activity (T/C of 36). The combination of the two drugs gave a T/C value of 26, which is significantly ($P < 0.001$) more than what was observed for bevacizumab alone (Fig. 1), whereas the difference between erlotinib and erlotinib þ bevacizumab did not reach significance ($P = 0.07$). It should be noted that in order to detect a meaningful difference between the agents when given alone or in combination, most studies were carried out with suboptimal doses of the two drugs.

Influence of *BRAF* status

The potent activity of erlotinib toward HT-29 xenografts was unexpected because HT-29 tumors show limited sensitivity to the EGFR-targeted antibody cetuximab (5). HT-29 cells express the *BRAF* V600E mutation (http://cancer.sanger.ac.uk/cosmic). To explore if the expression of mutant *BRAF* was associated with erlotinib sensitivity, we selected a different *BRAF* V600E-mutant cell line, CoLo205. However, the response of CoLo205 tumors to bevacizumab, erlotinib, and their combination (T/C values of 53, 64, and 32, respectively) was comparable with SW48 and SW620 rather than with HT-29 (Supplementary Fig. S1, bottom). Therefore, *BRAF* status as such cannot explain the unexpected erlotinib sensitivity of HT-29 xenografts.

Angiogenic signaling

Bevacizumab has preferential activity for human VEGF. To estimate the relative contribution of human tumor–derived and murine stromal-derived VEGF within the tumor microenvironment, tissue extracts were prepared from untreated SW48, HT-29, and SW620 tumors, and the concentration of murine and human VEGF was determined by species-specific ELISA analysis (data not shown). The results show that human VEGF represents more than 95% of the total VEGF in the tumor environment in agreement with previous findings (10, 12).

The microvascular density of SW48, HT-29, and SW620 xenografts was compared by immunohistochemistry with a CD31-directed antibody followed by quantitative image analysis. The results (Fig. 2, top left) indicate that bevacizumab reduced the microvascular density by rv65% in the bevacizumab-sensitive SW48 and SW620 xenografts compared with only rv30% in the bevacizumab-resistant HT-29 xenografts. In comparison, erlotinib treatment was accompanied by rv50% reduction of the vascular density in all 3 xenograft models. Interestingly, the addition of erlotinib to bevacizumab strongly diminished the microvascular density of HT-29 xenografts (from 30% to 64% of the vehicle control), suggesting that EGFR signaling contributes to the bevacizumab resistance of this tumor model. The combination of bevacizumab þ erlotinib was also significantly more effective than bevacizumab alone for the SW48 and SW620 tumor models, although the effect was less pronounced than for HT-29.

Bevacizumab exposure was accompanied by rv40% increased expression of tissue-associated VEGF that diminished significantly ($P < 0.01$) when erlotinib was added to bevacizumab (Fig. 2, top right). Most colorectal cancer cells and tumors express functional VEGFR1/Flt-1 that promotes cellular survival under environmental stress (13). Bevacizumab exposure was accompanied by increased levels of active phospho-VEGFR1 for all xenograft models which was attenuated ($P < 0.001$) by the addition of erlotinib (Fig. 2, middle right and bottom). This was most marked for the HT-29 xenografts where the levels of phospho-VEGFR1 were 171% in the presence of bevacizumab alone and 71% in the presence of bevacizumab þ erlotinib, compared with untreated vehicle controls. The differences in VEGFR1 phosphorylation were not linked to altered protein levels, as determined by ELISA of total VEGFR1 in tumor extracts (Supplementary Fig. S2). In

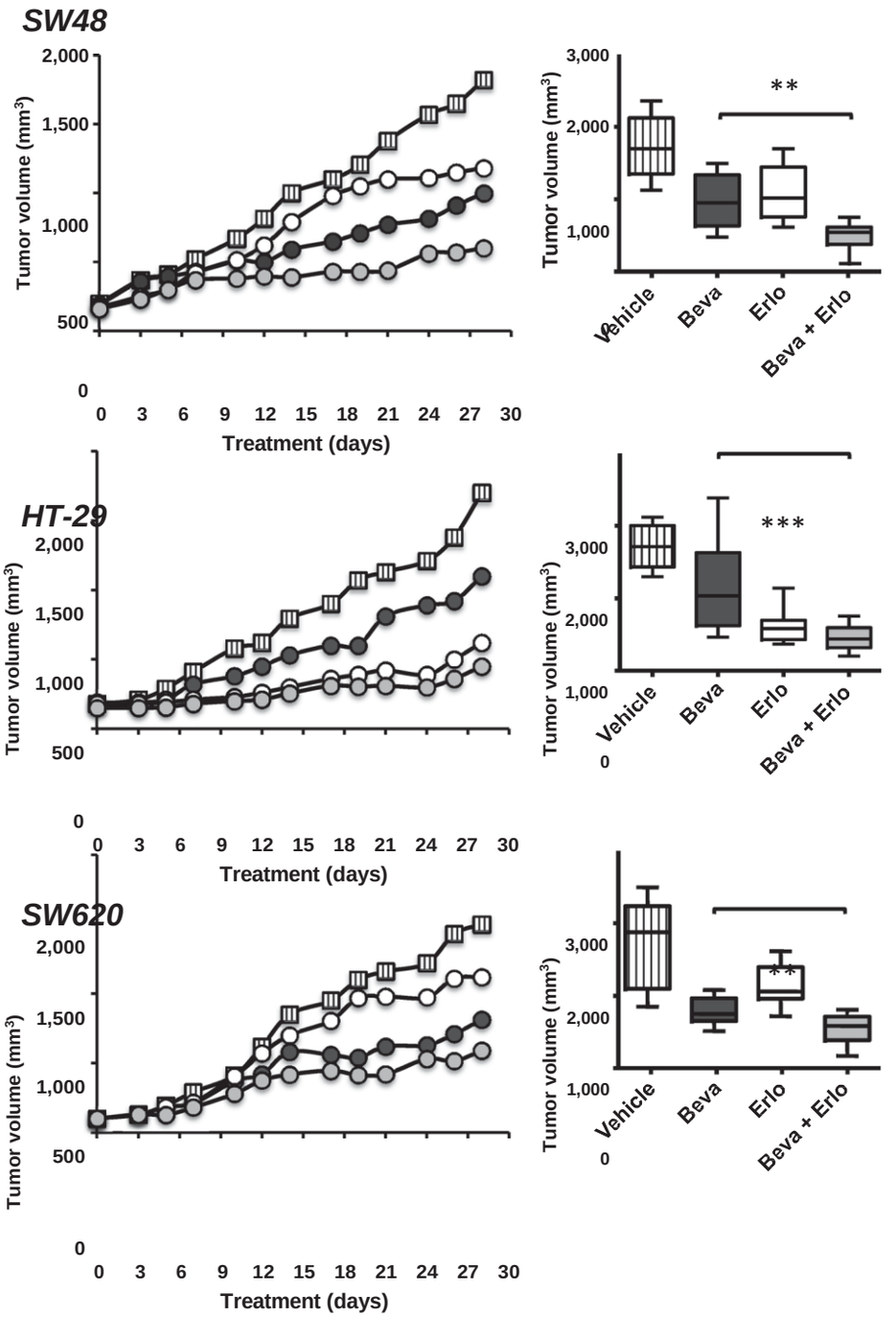

Figure 1.
Influence of bevacizumab, erlotinib, and their combination on tumor growth of colorectal cancer xenografts. Left, nude mice with SW48, HT-29, or SW620 colorectal cancer xenografts were dosed with vehicle (striped squares), bevacizumab (1 mg/kg i.p. every 3 days for SW48 and SW620 or 5 mg/kg i.p. every 3 days for HT-29; black circles), erlotinib (75 mg/kg p.o. once daily; white circles), or bevacizumab and erlotinib together (light gray circles). The curves represent the average tumor growth of at least 7 animals per group. Right, box and whisker plots of tumor volumes in mice with SW48, HT-29, or SW620 colorectal cancer xenografts after 4 weeks treatment with vehicle, bevacizumab (beva), erlotinib (erlo), or their combination (beva þ erlo). Lines, medians; boxes, 25th to 75th percentile interquartile ranges; whiskers, the highest and lowest value for a given treatment. The brackets indicate the difference between the bevacizumab groups and the corresponding bevacizumab þ erlotinib group. *P* values were calculated using the Student paired *t* test. **, $P < 0.01$; ***, $P < 0.001$.

bevacizumab-treated tumors, the active, autophosphorylated form of pVEGFR1 was mostly localized inside the cells as indicated by a prominent cytoplasmic signal (Fig. 2, bottom, indicated with a white arrow).

In addition to VEGFR1, colorectal cancer xenografts may express low levels of VEGFR2/Flk-1. Bevacizumab exposure was accompanied by up to 2-fold increase in the levels of phospho-VEGFR2 that was significantly attenuated in the presence of erlotinib, with the exception of the SW620 model, where the modest decrease did not reach significance (Fig. 2, middle right). It is noticeable that the levels of VEGFR1 and VEGFR2 protein are very different, with about 20-fold less VEGFR2, compared with VEGFR1, in SW48 and SW620 tumors and almost 80-fold less VEGFR2, compared with VEGFR1, in HT-29 xenografts (Supplementary Fig. S2). These differences may explain the current controversy concerning the expression of VEGFR2 by colorectal cancer cells (13). Taken together, our findings show that bevacizumab activates autocrine VEGF signaling in all three xenograft models which can be attenuated by erlotinib.

EGFR signaling

Next, the levels of total and phosphorylated EGFR were determined (Fig. 3, top). The results show that erlotinib exposure was accompanied by decreased levels of the active, autophosphorylated form of EGFR which was most pronounced for SW48 (66% inhibition, compared with the vehicle control) followed by

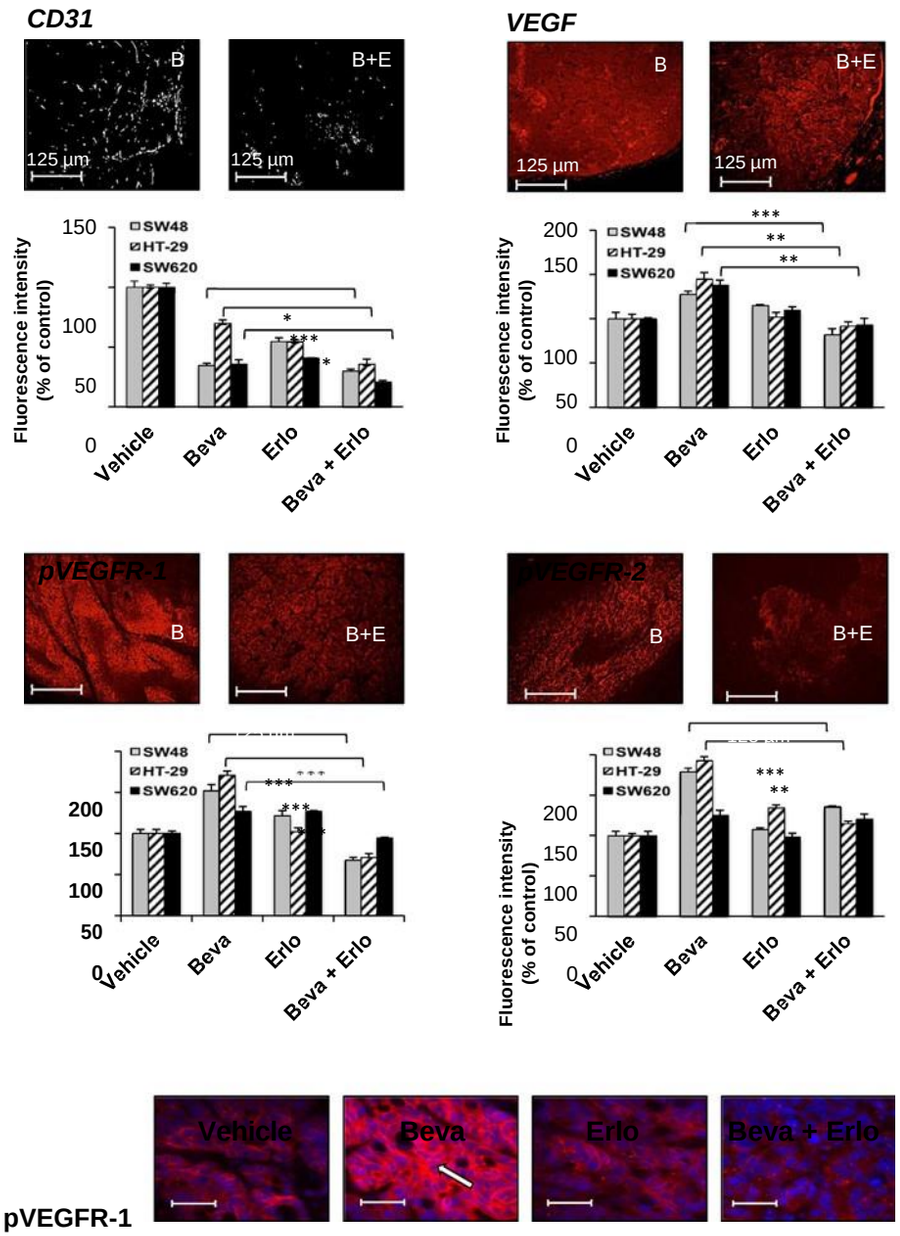

Figure 2.
Influence of bevacizumab, erlotinib, and their combination on tumor angiogenesis. Animals with SW48 (gray columns), HT-29 (hatched columns), or SW620 (black columns) human colorectal cancer xenografts were treated with bevacizumab (beva), erlotinib (erlo), or their combination (beva þ erlo) for 4 weeks as described in the legend to Fig. 1, followed by immunohistochemistry and quantitative image analysis. The photos illustrate the typical staining patterns for tumors derived from animals treated with bevacizumab (B) or with bevacizumab þ erlotinib (B þ E). For the microvascular density, CD31-positive endothelial blood vessels are outlined in white while the bar diagrams indicate the CD31-positive area, as a percentage of total, and represent the averages of at least 6 fields/tumor for at least 3 different tumors. For the quantitative analysis of VEGF, phospho-VEGFR1 and phospho-VEGFR2, the data represent the average fluorescence intensities of treated tumors compared with the treatment intensity of control tumors and are the averages of 6 fields/tumor for at least 3 different tumors. Bars, mean ± SEM. The brackets indicate the difference between the bevacizumab groups and the corresponding bevacizumab þ erlotinib groups. *P* values were calculated using the Student paired *t* test. *, $P < 0.05$; **, $P < 0.01$; ***, $P < 0.001$. Bottom, cellular distribution of phospho-VEGFR1 (pVEGFR1) after treatment with bevacizumab, erlotinib, and their combination in HT-29 tumors after 4 weeks treatment as described in the legend to Fig. 1. The presence of phospho-VEGFR1 was determined by immunohistochemistry and is indicated in red, whereas the nuclei appear in blue. The white arrow indicates the prominent intracellular accumulation of phosphorylated VEGFR1.

SW620 (50% inhibition) and HT-29 xenografts (35% inhibition). Unexpectedly, bevacizumab treatment was accompanied by strong EGFR activation ranging from rv140% for the bevacizumab-sensitive SW48 and SW620 xenografts to more than 200% for the bevacizumab-resistant HT-29 xenografts. The addition of erlotinib to bevacizumab was accompanied by a highly significant ($P < 0.001$) decrease in phospho-EGFR levels in all models shown by quantitative immunohistochemistry as well as by Western blot analysis (Fig. 3, top and middle). In comparison, bevacizumab had no detectable influence on total EGFR levels whereas erlotinib exposure, alone or in combination, was accompanied by a modest increase of total EGFR that never reached significance (Fig. 3 top and middle).

As observed for pVEGFR1, bevacizumab treatment was accompanied by a prominent cytoplasmic signal of pEGFR (Fig. 3, bottom, indicated with a white arrow).

EGFR signaling in endothelial cells

Tumor-associated endothelial cells (TEC) frequently express functional EGFR (14, 15). To characterize the expression of active EGFR on the TECs, a semiquantitative approach was developed as illustrated (Fig. 4, top left). Tumors were double-labeled for phospho-EGFR and CD31, and the degree of colocalization was determined as detailed in the figure legend. The results show that bevacizumab treatment was accompanied by a strong increase in TEC-associated phospho-EGFR while phospho-EGFR was

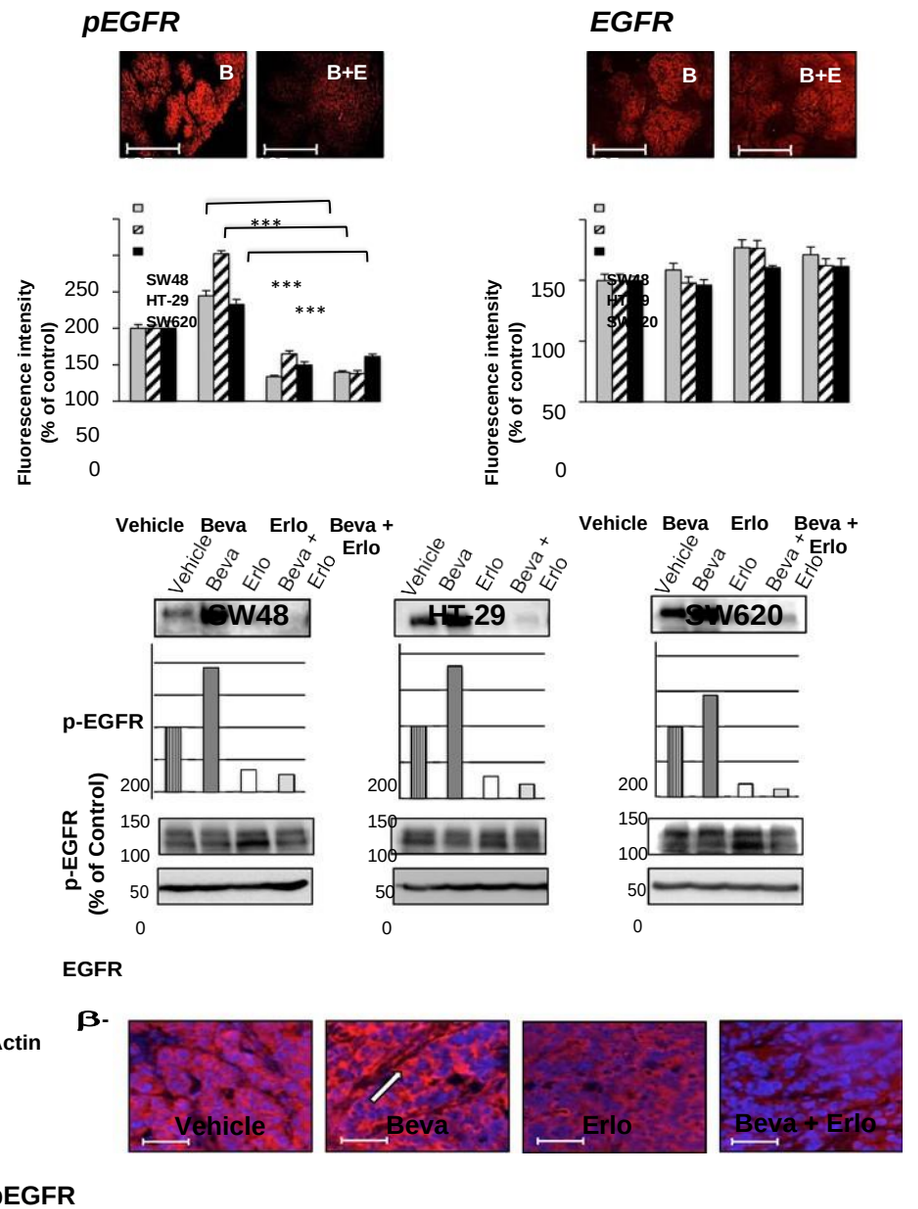

Figure 3.
Influence of bevacizumab, erlotinib, and their combination on EGFR. Animals with SW48 (gray columns), HT-29 (hatched columns), or SW620 (black columns) human colorectal cancer xenografts were treated with bevacizumab (beva), erlotinib (erlo), or their combination (beva þ erlo) for 4 weeks as described in the legend to Fig. 1. Top, the expression of phospho-EGFR and total EGFR was determined by immunohistochemistry followed by quantitative image analysis. The photos illustrate the typical staining patterns for tumors derived from animals treated with bevacizumab (B) or with bevacizumab þ erlotinib (B þ E). The bars indicate the mean ± SEM and represent the average fluorescence intensities of treated tumors compared with the treatment intensity of control tumors and are the averages of 6 fields/tumor for at least 3 different tumors. The brackets indicate the difference between the bevacizumab groups and the corresponding bevacizumab þ erlotinib groups. *P* values were calculated using the Student paired *t* test. *, $P < 0.05$; **, $P < 0.01$; ***, $P < 0.001$. Middle, Western blot analysis of pEGFR and EGFR expression in the tumors described above. The columns indicate the pEGFR signal (% of control) after normalization with b-actin that was used as loading control. Data represent typical results from 3 different experiments. Bottom, cellular distribution of phosphorylated EGFR (pEGFR) after treatment with bevacizumab, erlotinib, and their combination in HT-29 tumors after 4 weeks treatment as described in the legend to Fig. 1. The presence of phospho-EGFR was determined by immunohistochemistry and is indicated in red, whereas the nuclei appear in blue. The white arrow indicates the prominent intracellular accumulation of phosphorylated EGFR.

attenuated following treatment with erlotinib. Importantly, the addition of erlotinib to bevacizumab was associated with a highly significant ($P < 0.001$) decrease in TEC-associated phospho-EGFR, compared with bevacizumab alone, for all three xenograft models.

The EGFR ligands amphiregulin (AREG) and TGFa are known to form positive feedback loops with activated EGFR (16–18). Amphiregulin is of particular interest, because it is expressed at high levels in colorectal cancer and has potential predictive value for the response to EGFR-targeted agents (19, 20). Tumor extracts were prepared, and the ligand expression was determined by ELISA analysis. A modest increase in amphiregulin expression was observed in the bevacizumab-treated tumors while erlotinib treatment resulted in a rv50% decrease. Importantly, amphiregulin expression was significantly decreased in all bevacizumab þ erlotinib groups, compared with bevacizumab alone. For TGFa, the levels were too close to the detection limit to give reproducible results.

It has been reported that amphiregulin promotes endothelial tube formation *in vitro*, suggesting a direct role for amphiregulin in tumor angiogenesis (21). To determine if tumor-derived amphiregulin colocalize with the TECs, tumors were double-labeled for human amphiregulin and CD31. Unexpectedly, the results (Fig. 4, bottom) show prominent colocalization of amphiregulin and the TECs (indicated in yellow) compared with the more faint red labeling of amphiregulin in the tumor cells, coherent with a close *in vivo* association between the TECs and tumor-derived amphiregulin.

EGFR signaling in *RAS*-mutant cells

EGFR activation is accompanied by a positive feedback loop with some of its ligands, including TGFa and amphiregulin

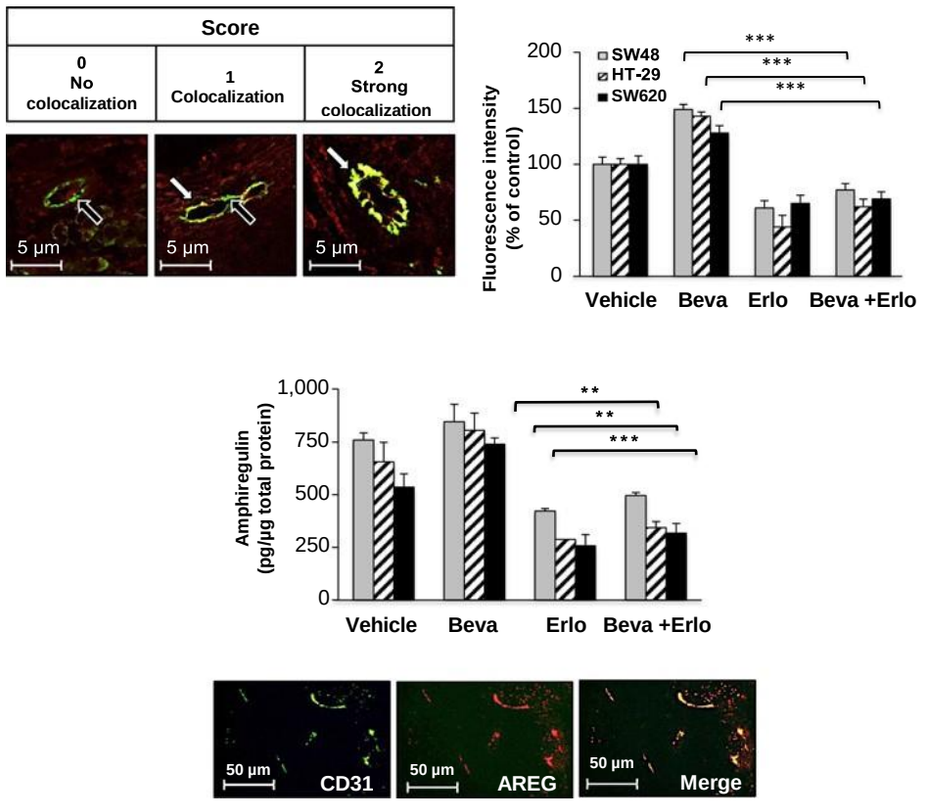

Figure 4.

EGFR signaling in TECs. Top, to identify phosphorylated EGFR on the TECs, double labeling was carried out for phospho-EGFR and CD31 and the degree of colocalization was determined by semiquantitative analysis as illustrated (top, left). Only blood vessels where the entire rim could be assessed were included in the analysis, with at least 12 blood vessels per group. For each blood vessel, no colocalization was characterized by a uniform green color (indicated with an open white arrow) and given a value of 0, some colocalization was characterized by a mixture of yellow and green cells and given a value of 1 and strong colocalization (indicated by a bold white arrow) was characterized by predominance of yellow cells and given a value of 2 thereby giving an estimate of the average levels of colocalization for each group. The results of the semiquantitative analysis are indicated in the top (right). *P* values were calculated using the Student paired *t* test. The brackets indicate the difference between the bevacizumab groups and the corresponding bevacizumab þ erlotinib groups. *P* values were calculated using the Student paired *t* test. *, $P < 0.05$; **, $P < 0.01$; ***, $P < 0.001$. Middle, animals with SW48 (gray columns), HT-29 (hatched columns) or SW620 (black columns) human CRC xenografts were treated with bevacizumab (beva), erlotinib (erlo) or their combination (beva þ erlo) for 4 weeks as described in the legend to Figure 1, and the expression of tumor-associated amphiregulin was determined by ELISA. The values represent the averages of 3 independent experiments, each done in duplicate. The brackets indicate the differences between bevacizumab and bevacizumab + erlotinib. P-values were calculated using Student paired t test. *, $P < 0.05$; **, $P < 0.01$; ***, $P < 0.001$. Bottom, to identify human, tumor-derived amphiregulin on the TECs, double labeling was carried out for CD31 (in green) and human amphiregulin (AREG in red) to visualize the degree of colocalization (merge, in yellow).

(16–18). Intriguingly, a recent study reports that EGFR-directed antibodies are unable to downregulate amphiregulin and TGFa in *RAS*-mutant colorectal cancer cells, which could, at least in part, explain the lack of activity of the mAbs toward such cells (11). The activity of erlotinib and cetuximab toward different *RAS*-mutant colorectal cancer cell lines was compared (Fig. 5). The results show that cetuximab exposure increased TGFa expression up to 4-fold in all cellular models, but had no significant influence on amphiregulin. In clear contrast, erlotinib decreased both TGFa and amphiregulin secretion, with highly significant ($P < 0.001$) differences between cetuximab and erlotinib in all cases (Fig. 5, top).

EGFR activation promotes tumor cell migration. Four colorectal cancer cell lines with good migratory capacity were selected, including LIM1215 (*RAS* WT), HCT-116, LS174T, and SW480 (all *RAS* mutant). EGF strongly stimulated the migration of all cell lines, which could be attenuated by erlotinib (Fig. 5, middle and bottom). In clear contrast, cetuximab was only able to attenuate migration of the *RAS* WT LIM1215 cells, without any detectable influence on the migration of the *RAS*-mutant cells. Importantly, the viability at the end of the incubation period was comparable for all groups (Supplementary Fig. S3).

Discussion

We here report that erlotinib increases the activity of bevacizumab in colorectal cancer models independent of *RAS* status and bevacizumab resistance. We further document differential activity of cetuximab and erlotinib on EGFR-mediated functions in colorectal cancer cells as a function of *RAS* status revealing fundamental differences between mAbs and TKIs targeting the same pathway. These findings inspired the DREAM phase III clinical trial (22) and provide the mechanistic framework to better understand why the

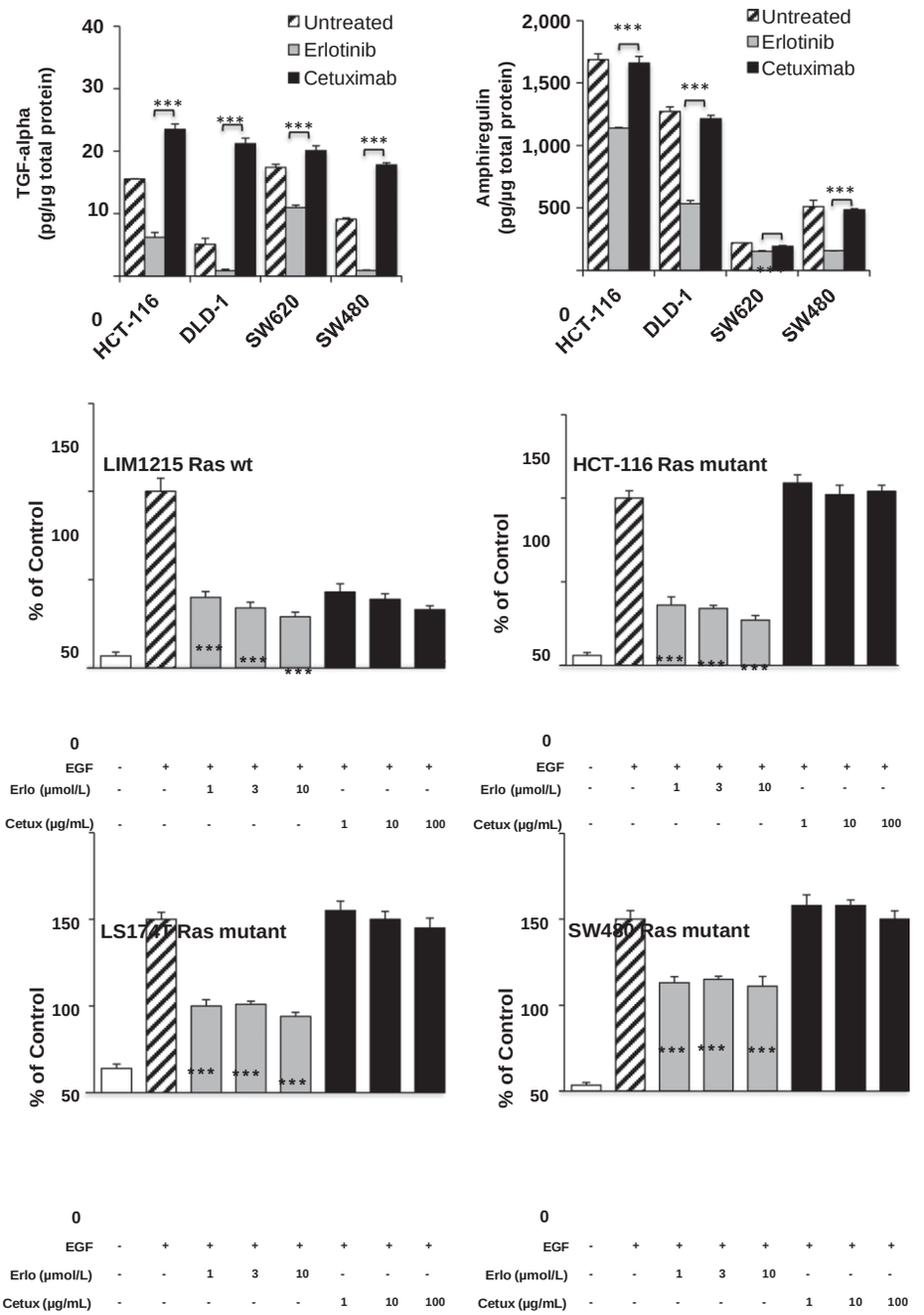

Figure 5.
Influence of erlotinib and cetuximab on EGFR signaling in colorectal cancer cells. Top, secretion of TGFa (left) or amphiregulin (right) in HCT-116, DLD-1, SW620, and SW480 cells after 72 hours incubation in the absence (hatched columns) or presence of erlotinib (3 mmol/L, gray columns) or cetuximab (1 mg/mL, black columns). The values represent the averages of 3 independent experiments, each done in duplicate. The brackets indicate the differences between erlotinib- and cetuximab-treated cells. Middle and bottom, migration of LIM1215, HCT-116, LS174T, and SW480 cells as determined by the Transwell assay (Boyden chamber) in the absence (white columns) or presence of EGF in the lower chamber and in the absence or presence of erlotinib (gray columns) or cetuximab (black columns) in the upper chamber. The values represent the averages of 3 independent experiments, each done in duplicate. The brackets indicate the difference between the positive EGF control and the erlotinib- or cetuximab-treated cells. *P* values were calculated using the Student paired *t* test. *, $P < 0.05$; **, $P < 0.01$; ***, $P < 0.001$.

bevacizumab þ erlotinib combination would be more active than bevacizumab alone.

Besides *RAS* status, there is increasing interest in the impact of primary tumor location. Current evidence suggests that metastatic colorectal cancer (mCRC) arising from different sides of the colon (left vs. right) have different clinical outcomes, which may, at least in part, be a reflection of the different embryonic origin of the normal tissue forming the left and right sides of the colon. In mCRC, patients with right-sided tumors have generally worse prognosis than those with left-sided tumors (23, 24). Furthermore, retrospective analysis of pooled clinical trials suggests that EGFR-targeted antibodies may be more active toward left-sided *RAS* WT tumors compared with right-sided *RAS* WT tumors (24–26). Interestingly, it has been reported that VEGF targeting may also differ between right- and left-sided tumors. In particular, bevacizumab may only provide a survival advantage for left-sided and rectal tumors (27, 28), suggesting that right- and left-sided tumors may respond differently to both EGFR- and VEGF-targeted anticancer agents. However, a large prospective trial is still needed to confirm these data.

Unfortunately, little is known about the origin of the vast majority of colorectal cancer cell lines including the ones used here. However, based on putative site-specific markers, it has been suggested that HT-29 is likely derived from a right-sided tumor while SW620 is likely derived from a left-sided tumor (29). Although the origin of these cell lines can never be determined with full certainly, it is tempting to speculate that erlotinib, alone or in combination with bevacizumab, may prove particularly interesting for treatment of patients with right-sided mCRC, a patient subgroup in need of novel, active agents.

Usually, EGFR inhibition is believed to principally influence tumor cells while VEGF targeting is acting on endothelial cells. The

.

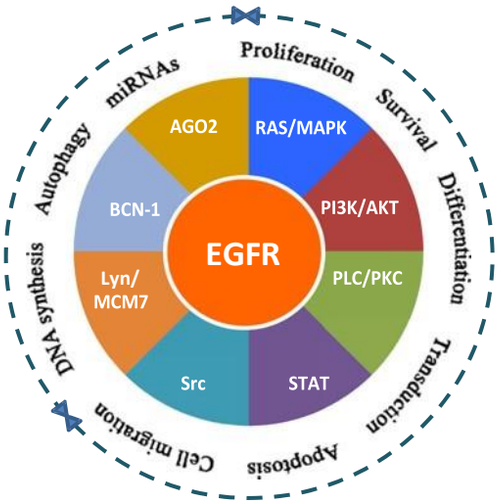

Figure 6.
Outline of classical and novel EGFR signaling pathways. EGFR mediates a wide variety of cellular functions including both classical mechanisms and newly identified pathways that plays a role in the regulation of DNA synthesis (Lyn/MCM7), autophagy (BCN-1), and miRNA processing (AGO2). The phosphorylation of AGO2 and Beclin1 is mediated by catalytically active EGFR present on intracellular vesicles after internalization, but before lysosomal degradation (34, 35).

results presented here provide evidence for a more complex model. Pruning of the tumor-associated microvasculature is accompanied by tumor cell hypoxia, activation of tumor-associated VEGF signaling as well as EGFR activation. In addition, vascular pruning interfered with tumor cell receptor recycling as evidenced by a prominent cytoplasmic signal for both pVEGFR1 and pEGFR in agreement with an influence of the oxygen-sensing pathway on endocytosis (30). Interestingly, bevacizumab exposure was also accompanied by EGFR signaling activation and accumulation of tumor-derived amphiregulin in the TECs. Taken together, these results suggest that both tumor cells and TECs are targeted by EGFR blockage.

The finding that an EGFR-targeted TKI may have different activity compared with EGFR-targeted antibodies *in vitro* as *in vivo* is initially surprising. However, it should be noted that the mAbs and the TKIs owe their activity to different mechanisms. Binding of the mAbs to EGFR is followed by endocytosis and lysosomal degradation, thereby decreasing receptor density on the cell surface (31). In the case of the TKIs, it is the catalytic activity of EGFR that is inhibited without an immediate effect on EGFR protein levels. Importantly, the activity of the TKIs is not restricted to surface-associated EGFR but includes additional pools of EGFR, like the active EGFR contained in endosomes following receptor internalization. Furthermore, recent results suggest that the interaction between EGFR and Ras proteins ceases within minutes after EGFR activation, with EGFR accumulating in the endosomes while Ras remain associated with the plasma membrane, thereby providing a physical separation between the two molecules and rapid signal downregulation (32).

Traditionally, EGFR signaling has been associated with canonical cellular signaling pathways like Ras/MAPK, PI3K/Akt, phospholipase C/PKC, STAT, and Src pathways as depicted in Fig. 6. However, several novel EGFR signaling pathways have been described recently including the binding of EGFR to and phosphorylation of the tyrosine kinase Lyn, which then phosphorylate MCM7, a licensing factor critical for DNA synthesis (33), beclin1 (BCN-1), a crucial mediator of autophagy (34), and argonaute 2 (AGO2) a modulator of microRNA processing (35). Importantly, the phosphorylation of AGO2 and Beclin1 is mediated by catalytically active EGFR present on intracellular vesicles after internalization, but before lysosomal degradation (34, 35), thereby representing a subfraction of EGFR that can only be inhibited by EGFR-directed small molecules, but not by EGFR-directed mAbs.

In conclusion, our study provides strong evidence that mAbs and TKIs target different elements of the EGFR signaling pathway, both as single agents and in combination with VEGF-targeted therapies. These findings may provide a rationale for novel therapeutic strategies for treatment of patient subgroups that are currently unlikely to benefit from EGFR-targeted antibodies. We further suggest that differential activity of mAbs and TKIs targeting the same signaling pathway is likely applicable for other tumor types.

Disclosure of Potential Conflicts of Interest

A. Savina is an employee of Institut Roche. B. Chibaudel is a consultant/advisory board member for Bayer, Lilly, Roche, and Sanofi. T. Andre reports receiving speakers bureau honoraria from and is a consultant/advisory board member for Roche. A.K. Larsen reports receiving commercial research support from Roche. No potential conflicts of interest were disclosed by the other authors.

Disclaimer

The sponsors had no role in the study design, data collection and analysis, interpretation of the results, the preparation of the manuscript, or the decision to submit the manuscript for publication.

Authors' Contributions

Conception and design: A. Savina, C. Tournigand, A. de Gramont, A.K. Larsen
Development of methodology: P. Mésange, A. Bouygues, A.K. Larsen
Acquisition of data (provided animals, acquired and managed patients, provided facilities, etc.): P. Mésange, N. Ferrand, A. Bouygues
Analysis and interpretation of data (e.g., statistical analysis, biostatistics, computational analysis): P. Mésange, A. Bouygues, N. Ferrand, A. Savina, B. Chibaudel, C. Tournigand, T. André, A. de Gramont, A.K. Larsen
Writing, review, and/or revision of the manuscript: P. Mésange, A. Bouygues, N. Ferrand, M. Sabbah, A.E. Escargueil, A. Savina, B. Chibaudel, C. Tournigand, T. André, A. de Gramont, A.K. Larsen
Administrative, technical, or material support (i.e., reporting or organizing data, constructing databases): M. Sabbah, A.E. Escargueil, A.K. Larsen
Study supervision: A. Savina, A.K. Larsen
Other (suggestions and technical advice): T. André

Acknowledgments

We thank Mériam Ayadi, Olivier Bernadini, Karima El Ouadrani, Virginie Megalophonos, Delphine Muller, Amélie Petitprez, and Virginie Poindessous

for help with the animal experiments. We appreciate the contribution of Tatiana Ledent from the animal facilities at Saint-Antoine Research Center and Sylvie Dumont and Fatiha Merabtene from the pathology platform at Hôpital Saint-Antoine.

This work was financed in part by research funding to A.K. Larsen from Roche. P. Mésange and A. Bouygues are generously supported by a Mouna Nasrallah fellowship.

The costs of publication of this article were defrayed in part by the payment of page charges. This article must therefore be hereby marked *advertisement* in accordance with 18 U.S.C. Section 1734 solely to indicate this fact.

Received October 26, 2017; revised January 9, 2018; accepted February 20, 2018; published first February 28, 2018.

References

1. Larsen AK, Ouaret D, El Ouadrani K, Petitprez A. Targeting EGFR and VEGF(R) pathway cross-talk in tumor survival and angiogenesis. Pharmacol Ther 2011;131:80–90.
2. Tabernero J. The role of VEGF and EGFR inhibition: implications for combining anti-VEGF and anti-EGFR agents. Mol Cancer Res 2007; 5:203–20.
3. Tol J, Koopman M, Cats A, Rodenburg CJ, Creemers GJ, Schrama JG, et al. Chemotherapy, bevacizumab, and cetuximab in metastatic colorectal cancer. N Engl J Med 2009;360:563–72.
4. Hecht JR, Mitchell E, Chidiac T, Scroggin C, Hagenstad C, Spigel D, et al. A randomized phase IIIB trial of chemotherapy, bevacizumab, and panitumumab compared with chemotherapy and bevacizumab alone for metastatic colorectal cancer. J Clin Oncol 2009;27:672–80.
5. Poindessous V, Ouaret D, El Ouadrani K, Battistella A, Mégalophonos VF, Kamsu-Kom N, et al. EGFR- and VEGF(R)-targeted small molecules show synergistic activity in colorectal cancer models refractory to combinations of monoclonal antibodies. Clin Cancer Res 2011;17:6522–30.
6. Lièvre A, Bachet JB, Boige V, Cayre A, Le Corre D, Buc E, et al. KRAS mutations as an independent prognostic factor in patients with advanced colorectal cancer treated with cetuximab. J Clin Oncol 2008; 26:374–9.
7. Douillard JY, Oliner KS, Siena S, Tabernero J, Burkes R, Barugel M, et al. Panitumumab-FOLFOX4 treatment and RAS mutations in colorectal cancer. N Engl J Med 2013;369:1023–34.
8. Atreya CE, Corcoran RB, Kopetz S. Expanded RAS: refining the patient population. J Clin Oncol 2015;33:682–5.
9. Ouaret D, Larsen AK. Protein kinase C b inhibition by enzastaurin leads to mitotic missegregation and preferential cytotoxicity toward colorectal cancer cells with chromosomal instability (CIN). Cell Cycle 2014;13: 2697–706.
10. Mésange P, Poindessous V, Sabbah M, Escargueil AE, de Gramont A, Larsen AK. Intrinsic bevacizumab resistance is associated with prolonged activation of autocrine VEGF signaling and hypoxia tolerance in colorectal cancer cells and can be overcome by nintedanib, a small molecule angiokinase inhibitor. Oncotarget 2014;5:4709–21.
11. Hobor S, Van Emburgh BO, Crowley E, Misale S, Di Nicolantonio F, Bardelli A. TGFa and amphiregulin paracrine network promotes resistance to EGFR blockade in colorectal cancer cells. Clin Cancer Res 2014;20: 6429–38.
12. Chiron M, Bagley RG, Pollard J, Mankoo PK, Henry C, Vincent L, et al. Differential antitumor activity of afflibercept and bevacizumab in patient-derived xenograft models of colorectal cancer. Mol Cancer Ther 2014;13: 1636–44.
13. Larsen AK, de Gramont A, Bouygues A, Ayadi M, Measange P. Functions and clinical implications of autocrine VEGF signaling in colorectal cancer. Curr Colorectal Cancer Rep 2013;9:270–27.
14. Yokoi K, Thaker PH, Yazici S, Rebhun RR, Nam DH, He J, et al. Dual inhibition of epidermal growth factor receptor and vascular endothelial growth factor receptor phosphorylation by AEE788 reduces growth and metastasis of human colon carcinoma in an orthotopic nude mouse model. Cancer Res 2005;65:3716–25.
15. Amin DN, Hida K, Bielenberg DR, Klagsbrun M. Tumor endothelial cells express epidermal growth factor receptor (EGFR) but not ErbB3 and are responsive to EGF and to EGFR kinase inhibitors. Cancer Res 2006;66: 2173–80.
16. Coffey RJ Jr, Derynck R, Wilcox JN, Bringman TS, Goustin AS, Moses HL, et al. Production and auto-induction of transforming growth factor-alpha in human keratinocytes. Nature 1987;328:817–20.
17. Gunaratnam L, Morley M, Franovic A, de Paulsen N, Mekhail K, Parolin DA, et al. Hypoxia inducible factor activates the transforming growth factor-alpha/epidermal growth factor receptor growth stimulatory pathway in VHL(-/-) renal cell carcinoma cells. J Biol Chem 2003; 278:44966–74.
18. Panupinthu N, Yu S, Zhang D, Zhang F, Gagea M, Lu Y, et al. Self-reinforcing loop of amphiregulin and Y-box binding protein-1 contributes to poor outcomes in ovarian cancer. Oncogene 2014;33:2846–56.
19. Khambata-Ford S, Garrett CR, Meropol NJ, Basik M, Harbison CT, Wu S, et al. Expression of epiregulin and amphiregulin and K-ras mutation status predict disease control in metastatic colorectal cancer patients treated with cetuximab. J Clin Oncol 2007;25:3230–7.
20. Salazar R, Capellà G, Tabernero J. Paracrine network: another step in the complexity of resistance to EGFR blockade? Clin Cancer Res 2014;20: 6227–9.
21. Bordoli MR, Stiehl DP, Borsig L, Kristiansen G, Hausladen S, Schraml P, et al. Prolyl-4-hydroxylase PHD2- and hypoxia-inducible factor 2-dependent regulation of amphiregulin contributes to breast tumorigenesis. Oncogene 2011;30:548–60.
22. Tournigand C, Chibaudel B, Samson B, Scheithauer W, Vernerey D, Mésange P, et al. Bevacizumab with or without erlotinib as maintenance therapy in patients with metastatic colorectal cancer (GERCOR DREAM; OPTIMOX3): a randomised, open-label, phase 3 trial. Lancet Oncol 2015;16:1493–1505.
23. Loupakis F, Yang D, Yau L, Feng S, Cremolini C, Zhang W, et al. Primary tumor location as a prognostic factor in metastatic colorectal cancer. J Natl Cancer Inst 2015;107.
24. Arnold D, Lueza B, Douillard JY, Peeters M, Lenz HJ, Venook A, et al. Prognostic and predictive value of primary tumour side in patients with RAS wild-type metastatic colorectal cancer treated with chemotherapy and EGFR directed antibodies in six randomised trials. Ann Oncol 2017;28: 1713–29.
25. Holch JW, Ricard I, Stintzing S, Modest DP, Heinemann V. The relevance of primary tumour location in patients with metastatic colorectal cancer: A meta-analysis of first-line clinical trials. Eur J Cancer 2017;70:87–98.
26. Cao DD, Xu HL, Xu XM, Ge W. The impact of primary tumor location on efficacy of cetuximab in metastatic colorectal cancer patients with different Kras status: a systematic review and meta-analysis. Oncotarget 2017;8: 53631–41.
27. Boisen MK, Johansen JS, Dehlendorff C, Larsen JS, Osterlind K, Hansen J, et al. Primary tumor location and bevacizumab effectiveness in patients with metastatic colorectal cancer. Ann Oncol 2013;24: 2554–9.
28. He WZ, Liao FX, Jiang C, Kong PF, Yin CX, Yang Q, et al. Primary tumor location as a predictive factor for first-line bevacizumab effectiveness in metastatic colorectal cancer patients. J Cancer 2017;8:388–94.
29. Bauer KM, Hummon AB, Buechler S. Right-side and left-side colon cancer follow different pathways to relapse. Mol Carcinog 2012;51:411–21.
30. Wang Y, Roche O, Yan MS, Finak G, Evans AJ, Metcalf JL, et al. Regulation of endocytosis via the oxygen-sensing pathway. Nat Med 2009;15:319–24.
31. Spangler JB, Neil JR, Abramovitch S, Yarden Y, White FM, Lauffenburger DA, et al. Combination antibody treatment down-regulates epidermal growth factor receptor by inhibiting endosomal recycling. Proc Natl Acad Sci U S A 2010;107:13252–7.
32. Pinilla-Macua I, Watkins SC, Sorkin A. Endocytosis separates EGF receptors from endogenous fluorescently labeled HRas and diminishes receptor

signaling to MAP kinases in endosomes. Proc Natl Acad Sci U S A 2016; 113:2122–7.

33. Huang TH, Huo L, Wang YN, Xia W, Wei Y, Chang SS, et al. Epidermal growth factor receptor potentiates MCM7-mediated DNA replication through tyrosine phosphorylation of Lyn kinase in human cancers. Cancer Cell 2013;23:796–810.
34. Wei Y, Zou Z, Becker N, Anderson M, Sumpter R, Xiao G, et al. EGFR-mediated Beclin 1 phosphorylation in autophagy suppression, tumor progression, and tumor chemoresistance. Cell 2013;154:1269–84.
35. Shen J, Xia W, Khotskaya YB, Huo L, Nakanishi K, Lim SO, et al. EGFR modulates microRNA maturation in response to hypoxia through phosphorylation of AGO2. Nature 2013;497:383–7.